Production of exotic charmonium in $\gamma\gamma$ interactions at hadron colliders

B. D. Moreira,[1] C. A. Bertulani,[2,3] V. P. Gonçalves,[4] and F. S. Navarra[1]

[1]*Instituto de Física, Universidade de São Paulo, C.P. 66318, São Paulo, São Paulo 05315-970, Brazil*
[2]*Department of Physics and Astronomy, Texas A&M University-Commerce, Commerce, Texas 75429, USA*
[3]*Department of Physics and Astronomy, Texas A&M University, College Station, Texas 77843, USA*
[4]*High and Medium Energy Group, Instituto de Física e Matemática, Universidade Federal de Pelotas Caixa Postal 354, Pelotas, Rio Grande do Sul 96010-900, Brazil*

(Received 21 October 2016; published 21 November 2016)

In this paper we investigate the exotic charmonium production in $\gamma\gamma$ interactions present in proton-proton, proton-nucleus, and nucleus-nucleus collisions at the CERN Large Hadron Collider energies as well as for the proposed energies of the Future Circular Collider. Our results demonstrate that the experimental study of these processes is feasible and can be used to constrain the theoretical decay widths and shed some light on the configuration of the considered multiquark states.

DOI: 10.1103/PhysRevD.94.094024

I. INTRODUCTION

Over the last years the existence of exotic hadrons has been firmly established [1–3] and now the next step is to accurately determine their structure. Among the proposed configurations, the meson molecule and the tetraquark are the most often discussed. The main difference between a tetraquark and a meson molecule is that the former is compact and the interaction between the constituents occurs through color exchange forces whereas the latter is an extended object and the interaction between its constituents happens through meson exchange forces. It is also possible that the observed states are charmonium-tetraquark, charmonium-molecule, or tetraquark-molecule mixtures. Indeed this mixed approach has led to the best description of the $X(3872)$. In Ref. [4] the mass and strong decay width were very well reproduced assuming that the $X(3872)$ has a $c\bar{c}$ component with a weight of 97% and a $D\overline{D}^*$ component with 3% weight. As for the production in proton-proton (pp) collisions, both at Fermilab and at the LHC, in Ref. [5] it was shown that the best description can be achieved with a charmonium-molecule combination, i.e., $\chi'_{c1} - D\overline{D}^*$, in which the $c\bar{c}$ component is of the order of 28%–44%. Even if the best description is given by a mixture it is still very important to understand the individual role played by each component.

One of the reactions that was proposed as a tool to discriminate between the two theoretical descriptions of the exotic states (R) is the decay into two photons, i.e., $R \to \gamma\gamma$. This process involves particle-antiparticle annihilation, which is sensitive to the spatial configuration of the decaying states and should be hindered if its constituents are away from each other, as is the case in a molecular configuration. In fact, for an S-wave nonrelativistic two-body system R in a state described by a wave function $\psi(r)$, the width for annihilation into $\gamma\gamma$ is given by

$$\Gamma(R \to \gamma\gamma) = \frac{2\pi\alpha^2}{M_R^2}|\psi(0)|^2. \tag{1}$$

We may expect that for a loosely bound meson molecule $|\psi(0)|^2$ is much smaller than for a diquark-antidiquark compact system.

The production of exotic particles in hadronic colliders is one of the most promising testing grounds for our ideas about the structure of the new states. It has been shown [2,6,7] that it is difficult to produce molecules in pp collisions. In a pure molecular approach the estimated cross section for $X(3872)$ production is 2 orders of magnitude smaller than the measured one. One might try to explain these data with a pure tetraquark model. An attempt to do this, using an extension of the color evaporation model to the cases where we have double parton scattering, was presented in [8]. An alternative is to explore the fact that ultrarelativistic hadrons are an intense source of photons (for a review see Ref. [9–14]) and investigate resonance production in the $\gamma\gamma$ and γh (h = p, A) interactions present in pp/pA/AA collisions. At large impact parameters ($b > R_{h_1} + R_{h_2}$), denoted hereafter ultraperipheral collisions (UPCs), the photon-induced interactions become dominant with the final state being characterized by the state R and the presence of one intact hadron, in the case of an inclusive γh interaction, or two intact hadrons if the resonance was produced in a $\gamma\gamma$ or a diffractive γh interaction. Recent experimental results at the RHIC [15,16], Tevatron [17], and LHC [18–26] have demonstrated that the study of photon-induced interactions in hadronic collisions is feasible and can be used to improve our understanding of the QCD dynamics as well as to probe beyond standard model physics (see, e.g., Refs. [27–29]). In this work we systematically explore the possibility of producing exotic charmonium in two-photon interactions in UPCs with ultrarelativistic protons and nuclei. We consider

hadronic collisions at the LHC as well as in the proposed Future Circular Collider (FCC) [30].

The idea of studying exotic meson production in UPCs was pioneered in [31], where the production cross section of several light and heavy well-known mesons (and also exotic mesons and glueballs candidates) in nucleus-nucleus collisions was computed. Later, in Ref. [32], the same formalism was applied to the production of mesons and exotic states in proton-proton collisions. Special attention was given to the exotic charmonium states $X(3940)$ and $X(4140)$. More recently, in Ref. [33], the authors calculated the cross sections of the processes $pp \to pnX$, where X are the exotic charmonium states $Z_c(3900)$, $Z(4430)$, $X(3940)$, and $X(3915)$. In these reactions one proton emits one photon and the other emits a pion or a pomeron.

In this work we revisit and update the calculations performed in [31] and [32], extending them to pp, pA, and AA collisions at LHC and FCC energies. We focus on photon-photon production of the exotic charmonium states and include $X(3915)$, $Z(3930)$, and $X(4160)$. As it will be seen, all the ingredients of the calculation are fixed with the exception of the two-photon decay width of the exotic state (1). In principle, tetraquark and molecular configurations would yield quite different numbers for the decay widths, which would yield quite different production cross sections. The two-photon decay width of the exotic states has been calculated in the molecular approach in several works [34–37]. Unfortunately, the theoretical predictions of the tetraquark model are not yet available. We present production cross sections of meson molecules keeping in mind that, if the states in question were tetraquarks, the corresponding cross sections would be much larger.

This paper is organized as follows. In Sec. II we present a short description of the formalism used for particle production in $\gamma\gamma$ interactions at hadronic colliders. In Sec. III we present our predictions for the exotic charmonium production in pp/pA/AA collisions at LHC and FCC energies. Finally, in Sec. IV we summarize our main conclusions.

II. FORMALISM

Since the theoretical treatment of UPCs in relativistic heavy ion collisions has been extensively discussed in the literature [9–14], in what follows we only review the main formulas needed to make predictions for exotic meson production in $\gamma\gamma$ interactions. In the equivalent photon approximation, the cross section for the production of a generic exotic charmonium state, X, in UPCs between two hadrons, h_1 and h_2, is given by (see, e.g., [9,13])

$$\begin{aligned}\sigma(h_1h_2 \to h_1 \otimes R \otimes h_2; s) &= \int \hat{\sigma}(\gamma\gamma \to R; W) N(\omega_1, \mathbf{b}_1) \\ &\times N(\omega_2, \mathbf{b}_1) S^2_{abs}(\mathbf{b}) \mathrm{d}^2\mathbf{b}_1 \mathrm{d}^2\mathbf{b}_2 \mathrm{d}\omega_1 \mathrm{d}\omega_2, \end{aligned} \tag{2}$$

where $\sqrt{s}$ is the center-of-mass energy for the h_1h_2 collision (h_i = p, A), $\otimes$ characterizes a rapidity gap in the final state, and $W = \sqrt{4\omega_1\omega_2}$ is the invariant mass of the $\gamma\gamma$ system. Moreover, $N(\omega_i, b_i)$ is the equivalent photon spectrum generated by hadron (nucleus) i, and $\sigma_{\gamma\gamma\to R}(\omega_1, \omega_2)$ is the cross section for the production of a state R from two real photons with energies ω_1 and ω_2. Moreover, in Eq. (2), ω_i is the energy of the photon emitted by the hadron (nucleus) h_i at an impact parameter, or distance, b_i from h_i. The photons, and their corresponding electric fields, interact at the point shown in Fig. 1. The factor $S^2_{abs}(\mathbf{b})$ is the absorption factor, given in what follows by [38]

$$\begin{aligned} S^2_{abs}(\mathbf{b}) &= \Theta(|\mathbf{b}| - R_{h_1} - R_{h_2}) \\ &= \Theta(|\mathbf{b}_1 - \mathbf{b}_2| - R_{h_1} - R_{h_2}), \end{aligned} \tag{3}$$

where R_{h_i} is the radius of the hadron h_i ($i = 1, 2$). The presence of this factor in Eq. (2) excludes the overlap between the colliding hadrons and allows us to take into account only ultraperipheral collisions. Remembering that the photon energies ω_1 and ω_2 are related to W, and the rapidity Y of the outgoing resonance R is related by

$$\omega_1 = \frac{W}{2} e^Y \quad \text{and} \quad \omega_2 = \frac{W}{2} e^{-Y}, \tag{4}$$

the total cross section can be expressed by (for details see, e.g., Ref. [39])

$$\begin{aligned}\sigma(h_1h_2 \to h_1 \otimes R \otimes h_2; s) &= \int \hat{\sigma}(\gamma\gamma \to R; W) N(\omega_1, \mathbf{b}_1) N(\omega_2, \mathbf{b}_2) \\ &\times S^2_{abs}(\mathbf{b}) \frac{W}{2} \mathrm{d}^2\mathbf{b}_1 \mathrm{d}^2\mathbf{b}_2 \mathrm{d}W \mathrm{d}Y. \end{aligned} \tag{5}$$

The equivalent photon flux can be expressed as follows,

$$N(\omega, b) = \frac{Z^2\alpha_{em}}{\pi^2} \frac{1}{b^2\omega} \left[\int u^2 J_1(u) F\left(\sqrt{\frac{(b\omega/\gamma)^2 + u^2}{b^2}} \right) \times \frac{1}{(b\omega/\gamma)^2 + u^2} \mathrm{d}u \right]^2, \tag{6}$$

where F is the nuclear form factor of the equivalent photon source. In the nuclear case, it is often used in the literature as a monopole form factor given by [39]

$$F(q) = \frac{\Lambda^2}{\Lambda^2 + q^2}, \tag{7}$$

with $\Lambda = 0.088$ GeV. For proton projectiles, the form factor is in general assumed to be [40,41]

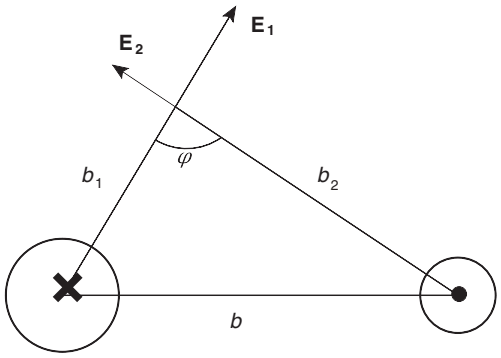

FIG. 1. Electromagnetic field interaction in ultraperipheral hadron-hadron (or nucleus-nucleus) collisions. The particle on the left moves into the page and the particle on the right moves out of the page. They are separated by the impact parameter b.

$$F(q) = 1/[1 + q^2/(0.71\ \mathrm{GeV}^2)]^2. \quad (8)$$

In what follows we assume these form factors to estimate the cross sections. However, as discussed in detail in Ref. [39], distinct models for F imply that the resulting cross sections can differ significantly. In order to estimate the theoretical uncertainty associated to the model used for F, in what follows we also present the predictions obtained assuming $F(q) = 1$, i.e., that the proton and nucleus are pointlike particles. In this case, we need to integrate from a minimum distance $b_i = R_i$ ($\sim$0.7 fm for protons and $1.2A^{1/3}$ fm for nuclei) in Eq. (2), because the flux is divergent for $b = 0$ [31,42]. Additionally, in the case of $PbPb$ collisions, we also consider a more realistic form factor, obtained as a Fourier transform of the Woods-Saxon distribution for the nuclear density. As demonstrated in Ref. [39], this form factor coincides with the monopole one only in a very limited range of values of the photon virtuality, with the difference between them becoming larger at large values of q.

In order to estimate the $h_1h_2 \to h_1 \otimes R \otimes h_2$ cross section we need the $\gamma\gamma \to R$ interaction cross section as input. In what follows we use the Low formula [43], where the cross section for the production of the R state due to the two-photon fusion can be written in terms of the two-photon decay width of the corresponding state as

$$\sigma_{\gamma\gamma\to R}(\omega_1, \omega_2) = 8\pi^2(2J+1)\frac{\Gamma_{R\to\gamma\gamma}}{M_R}\delta(4\omega_1\omega_2 - M_R^2), \quad (9)$$

where the decay width $\Gamma_{R\to\gamma\gamma}$ can in some cases be taken from experiment or can be theoretically estimated. Furthermore, M_R and J are, respectively, the mass and spin of the produced state. Finally, it is important to emphasize that due to the Z^2 dependence of the photon spectra, we have that for the same W the following hierarchy is expected to be valid for the resonance production induced by $\gamma\gamma$ interactions: $\sigma_{AA} = Z^2 \cdot \sigma_{pA} = Z^4 \cdot \sigma_{pp}$.

III. RESULTS

In this section we present our predictions for the production of exotic mesons due to photon-photon fusion in UPCs at energies available at the LHC and proposed for the FCC. We have considered all the charmonium states for which either a measurement or a theoretical estimate of the decay width is available. For the sake of comparison with the results found in [33] we consider the two possible assignments, 0^{++} and 2^{++}, for the states $X(3940)$ and $X(4140)$. In fact, in the last edition of the PDG [44] these states still appear with undefined assignments. The masses and decay widths were inferred from Refs. [34–36]. We use the following notation: $\sigma_{b_{\mathrm{min}}}$ denotes cross sections evaluated with $F = 1$, and σ_F denotes cross sections evaluated with the form factors from Eqs. (7) and (8) for nuclei and protons, respectively. In the particular case of $PbPb$ collisions we also present the predictions obtained using the realistic form factor [39], which we denote by σ_R. The precise form of the form factor is the main source of uncertainties in our calculations and the use of the two cases mentioned above gives us an estimate of the theoretical error.

Initially let us consider the energy dependence of the total cross sections and the rapidity distributions of the resonances produced in $\gamma\gamma$ interactions in UPCs. These observables were shown to be the most useful ones to be compared with theoretical predictions. This expectation has been confirmed by recent experimental results (obtained at the RHIC and also at the LHC) on vector meson production (ρ, J/Ψ, and Υ) [15–26]. Here we propose extending these measurements beyond the production of well-established mesons, such as the J/Ψ, and use UPCs in hadronic colliders to assess new information on exotic mesons and constrain theoretical predictions. In Fig. 2(a), we present our predictions for the energy dependence of the production cross section in Pb-Pb collisions with $\sqrt{s}$ from 100 GeV to 100 TeV obtained using the monopole form factors and the widths presented in Table I. Similar energy dependences are predicted for p-Pb and p-p collisions, with the normalization scaled by a factor $\approx 1/Z^2$ and $\approx 1/Z^4$, respectively. The predicted cross sections for the LHC kinematical range are of the order of 1–100 μb. Moreover, this result shows us that the cross sections are 1 order of magnitude larger for the energies expected to be covered by the FCC in Pb-Pb collisions ($\sqrt{s} = 39$ TeV). In Fig. 2(b), we show the rapidity distribution of the exotic charmonium production in Pb-Pb collisions at $\sqrt{s} = 5.5$ TeV. We have that the maximum of the distribution occurs at central rapidities, strongly decreasing at forward and backward rapidities. In particular, for the $X(4140)$ production, the two predictions differ by a factor 3 at $Y = 0$.

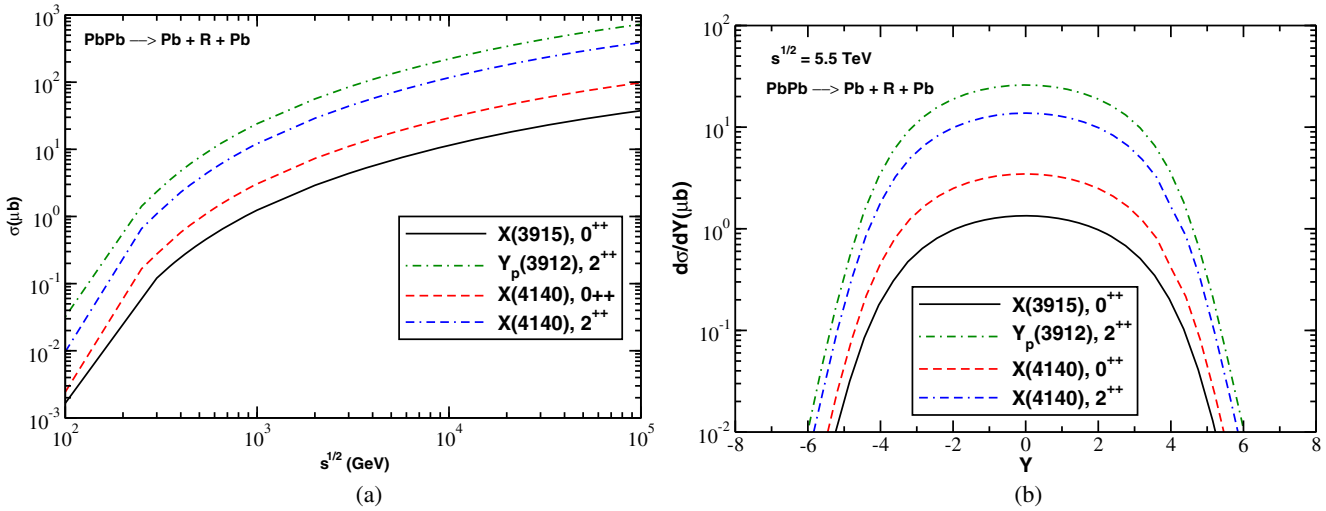

FIG. 2. (a) Cross section of the process PbPb → Pb ⊗ R ⊗ Pb as a function of the energy $\sqrt{s}$. (b) Rapidity distribution of the resonance produced in $\gamma\gamma$ interactions in Pb-Pb collisions at $\sqrt{s} = 5.5$ TeV.

In Tables I–III we present our predictions for the exotic charmonium production in Pb-Pb, p-Pb, and p-p collisions, respectively, using the form factors mentioned in the previous section. Owing to the form of the cross section of Eq. (2) and its dependence on the equivalent photon spectrum (6), the Pb-Pb cross sections are enhanced by a factor $Z^4(Z^2)$ in comparison to p-p (p-Pb) collisions. This is reflected in our calculations, with the cross sections ranging from a few hundred nb up to hundreds of μb.

In Table I we present our predictions for the cross sections for the production of several exotic mesons in Pb-Pb collisions at $\sqrt{s} = 2.76$ TeV, $\sqrt{s} = 5.5$ TeV, and $\sqrt{s} = 39$ TeV. Comparing the cross sections for different form factors we observe that $\sigma_F \approx 1.5\sigma_{b_{\rm min}}$. This happens because $\sigma_{b_{\rm min}}$ does not take into account meson production in the region $b_i < R_i$, while σ_F allows for this, as long as the constraint $b > R_1 + R_2$ is respected. Since the masses of the exotic states are nearly the same (within 5%), the main sources of changes in the cross sections are the magnitude of the decay width and the spin of the produced particle. The predicted cross sections are of the order of μb, and increase with the energy, as expected from Fig. 2. We can see that the predictions for the $X(3940)$ differ by a factor 4, depending on the spin assumed for the particle. Similar differences are predicted in the case of $X(4140)$ production. An important aspect is that the predictions for the production of the $X(3915)$ and $Y_p(3912)$ differ by a factor 20. Currently, it is not clear if these states are the same or not. Consequently, our results indicate that the study of their production in UPCs can be useful to constrain their main characteristics.

In Table II, we present our results for the production of exotic mesons in p-Pb collisions at $\sqrt{s} = 5$, 8.8, and 63 TeV. In this case we can observe that the differences between the predictions obtained with $\sigma_{b_{\rm min}}$ and σ_F are smaller than in the Pb-Pb case. This occurs because the effects of meson production in the region $b_i < R_i$, calculated with Eq. (8) are attenuated by the fact that the proton has a smaller radius than the Pb. Furthermore, in this case, the cross section is enhanced by a factor Z^2 in comparison to the p-p one, leading to cross sections that can only reach

TABLE I. Cross sections for exotic meson production in Pb-Pb collisions using the theoretical decay rates presented in Refs. [34–36].

			$\sigma_{b_{\rm min}}$ (μb)			σ_F (μb)			σ_R (μb)		
State	Mass	$\Gamma^{\rm theor}_{\gamma\gamma}$ (keV)	2.76 TeV	5.5 TeV	39 TeV	2.76 TeV	5.5 TeV	39 TeV	2.76 TeV	5.5 TeV	39 TeV
$X(3940)$, 0^{++}	3943	0.33	4.2	8.2	31.6	6.5	11.8	40.9	5.7	10.8	39.6
$X(3940)$, 2^{++}	3943	0.27	17.2	33.6	129.2	26.5	48.4	167.4	23.4	44.2	162.0
$X(4140)$, 0^{++}	4143	0.63	6.5	12.9	51.2	10.2	18.7	65.7	9.0	17.1	63.6
$X(4140)$, 2^{++}	4143	0.50	26.0	51.2	201.0	40.3	74.3	260.6	35.5	67.7	252.3
$Z(3930)$, 2^{++}	3922	0.083	5.4	10.5	40.9	8.3	15.2	52.4	7.4	13.9	50.5
$X(4160)$, 2^{++}	4169	0.363	18.4	36.4	144.2	28.6	52.7	185.3	25.2	48.1	178.7
$Y_p(3912)$, 2^{++}	3919	0.774	50.5	98.6	382.4	77.9	142.2	490.1	68.9	129.9	473.7
$X(3915)$, 0^{++}	3919	0.20	2.6	5.1	19.8	4.0	7.3	25.3	3.6	6.7	24.5

TABLE II. Cross sections for exotic meson production in p-Pb collisions using the theoretical decay rates presented in Refs. [34–36].

State	Mass	$\Gamma_{\gamma\gamma}^{\text{theor}}$ (keV)	$\sigma_{b_{\min}}$ (nb)			σ_F (nb)		
			5 TeV	8.8 TeV	63 TeV	5 TeV	8.8 TeV	63 TeV
$X(3940)$, 0^{++}	3943	0.33	2.8	4.0	10.6	3.3	4.5	11.3
$X(3940)$, 2^{++}	3943	0.27	11.4	16.3	43.4	12.9	18.3	46.3
$X(4140)$, 0^{++}	4143	0.63	4.4	6.3	16.6	5.0	7.1	18.3
$X(4140)$, 2^{++}	4143	0.50	17.6	25.2	65.9	20.0	28.4	72.5
$Z(3930)$, 2^{++}	3922	0.083	3.6	5.1	13.2	4.0	5.7	14.5
$X(4160)$, 2^{++}	4169	0.363	12.5	17.9	46.9	14.2	20.1	63.3
$Y_p(3912)$, 2^{++}	3919	0.774	33.5	47.7	123.3	37.9	53.6	132.0
$X(3915)$, 0^{++}	3919	0.20	1.7	2.5	6.4	2.0	2.8	7.0

TABLE III. Cross sections for exotic meson production in pp collisions using the theoretical decay rates presented in Refs. [34–36].

State	Mass	$\Gamma_{\gamma\gamma}^{\text{theor}}$(keV)	$\sigma_{b_{\min}}$ (pb)			σ_F (pb)		
			7 TeV	14 TeV	100 TeV	7 TeV	14 TeV	100 TeV
$X(3940)$, 0^{++}	3943	0.33	0.98	1.3	2.8	1.0	1.5	2.8
$X(3940)$, 2^{++}	3943	0.27	4.0	5.6	11.4	4.1	5.7	11.6
$X(4140)$, 0^{++}	4143	0.63	1.6	2.2	4.5	1.6	2.2	4.6
$X(4140)$, 2^{++}	4143	0.50	6.2	8.7	18.0	6.4	8.9	18.3
$Z(3930)$, 2^{++}	3922	0.083	1.2	1.7	3.6	1.3	1.8	3.6
$X(4160)$, 2^{++}	4169	0.363	4.4	6.1	12.8	4.5	6.3	13.0
$Y_p(3912)$, 2^{++}	3919	0.774	11.7	16.3	33.4	12.0	16.7	34.0
$X(3915)$, 0^{++}	3919	0.20	0.60	0.84	1.7	0.62	0.86	1.8

a few tens of nb. The differences between the different predictions, observed in the $A-A$ case, also are present in p-Pb collisions.

In Table III we present our results for the production of exotic mesons in p-p collisions at $\sqrt{s}=7$, 14, and 100 TeV. Here we observe a smaller difference between the two choices of form factor when compared with the previous cases. Moreover, in this case ($Z=1$) we do not have any enhancement of the cross section compared with the other cases, leading to much smaller cross sections. Even so, these are non-negligible cross sections, of the order of a few pb, well within the reach of present experimental detection techniques, considering the high luminosity present in pp collisions.

Before concluding, let us compare our predictions for the production of the $X(3915)$ and $X(3940)$ states in $\gamma\gamma$ interactions with those obtained in Ref. [33], where the contribution associated to γh interactions in pp collisions was estimated. We observe that the cross sections obtained in Ref. [33] are of the order of nb, while our predictions, presented in Table III, are of the order of pb. Therefore, the dominant channel for the production of these states is γh interactions. However, as demonstrated in Ref. [33], they are produced in the very forward region, with a large background associated to the Pomeron exchange, which makes the experimental separation of these states a hard task. In contrast, in $\gamma\gamma$ interactions, they produced essentially at central rapidities as shown in Fig. 2(b), i.e., in the kinematical range covered by the current LHC detectors.

IV. CONCLUSIONS

In this work we have studied the production of exotic mesons in UPCs at LHC and FCC energies due to two-photon fusion. This is a clean process where the particles of the initial state are intact at the final state and can be detected at the forward direction as featured by the presence of two rapidity gaps between the projectiles and the produced particle. Moreover, we have predicted large values for the cross sections in PbPb and pPb collisions and non-negligible values in pp collisions. Our predictions for the rapidity distributions can also be of relevance for testing the theoretical models used in the calculations. Therefore, we conclude that the experimental study is worth pursuing, that it can be useful to constrain decay widths evaluated theoretically and, ultimately, it can help in determining the configuration of the considered multiquark states.

ACKNOWLEDGMENTS

This work was partially financed by the Brazilian funding agencies CNPq, CAPES, FAPERGS, and FAPESP. This work was supported in part by the U.S. DOE Award No. DE- FG02-08ER41533 and the U.S. NSF Grant No. 1415656.

[1] A. Hosaka, T. Iijima, K. Miyabayashi, Y. Sakai, and S. Yasui, Prog. Theor. Exp. Phys. **2016**, 062C01 (2016).
[2] A. Esposito, A. L. Guerrieri, F. Piccinini, A. Pilloni, and A. D. Polosa, Int. J. Mod. Phys. A **30**, 1530002 (2015).
[3] M. Nielsen and F. S. Navarra, Mod. Phys. Lett. A **29**, 1430005 (2014); M. Nielsen, F. S. Navarra, and S. H. Lee, Phys. Rep. **497**, 41 (2010); F. S. Navarra, M. Nielsen, and S. H. Lee, Phys. Lett. B **649**, 166 (2007).
[4] R. D. Matheus, F. S. Navarra, M. Nielsen, and C. M. Zanetti, Phys. Rev. D **80**, 056002 (2009).
[5] C. Meng, H. Han, and K. T. Chao, arXiv:1304.6710.
[6] C. Bignamini, B. Grinstein, F. Piccinini, A. D. Polosa, and C. Sabelli, Phys. Rev. Lett. **103**, 162001 (2009).
[7] A. Esposito, A. L. Guerrieri, L. Maiani, F. Piccinini, A. Pilloni, A. D. Polosa, and V. Riquer, Phys. Rev. D **92**, 034028 (2015).
[8] F. Carvalho, E. R. Cazaroto, V. P. Gonçalves, and F. S. Navarra, Phys. Rev. D **93**, 034004 (2016).
[9] C. A. Bertulani and G. Baur, Phys. Rep. **163**, 299 (1988).
[10] C. A. Bertulani and G. Baur, Phys. Today **47**, No. 03, 22 (1994).
[11] C. A. Bertulani, S. Klein, and J. Nystrand, Annu. Rev. Nucl. Part. Sci. **55**, 271 (2005).
[12] A. J. Baltz, G. Baur, D. d'Enterria, L. Frankfurt, F. Gelis, V. Guzey, K. Hencken, Yu. Kharlov, M. Klasen, and S. R. Klein, Phys. Rep. **458**, 1 (2008).
[13] G. Baur, K. Hencken, and D. Trautmann, J. Phys. G **24**, 1657 (1998).
[14] G. Baur, K. Hencken, D. Trautmann, S. Sadovsky, and Y. Kharlov, Phys. Rep. **364**, 359 (2002).
[15] C. Adler *et al.* (STAR Collaboration), Phys. Rev. Lett. **89**, 272302 (2002).
[16] S. Afanasiev *et al.* (PHENIX Collaboration), Phys. Lett. B **679**, 321 (2009).
[17] T. Aaltonen *et al.* (CDF Collaboration), Phys. Rev. Lett. **102**, 242001 (2009).
[18] B. Abelev *et al.* (ALICE Collaboration), Phys. Lett. B **718**, 1273 (2013).
[19] E. Abbas *et al.* (ALICE Collaboration), Eur. Phys. J. C **73**, 2617 (2013).
[20] R. Aaij *et al.* (LHCb Collaboration), J. Phys. G **40**, 045001 (2013).
[21] R. Aaij *et al.* (LHCb Collaboration), J. Phys. G **41**, 055002 (2014).
[22] R. Aaij *et al.* (LHCb Collaboration), J. High Energy Phys. 09 (2015) 084.
[23] S. Chatrchyan *et al.* (CMS Collaboration), J. High Energy Phys. 01 (2012) 052.
[24] S. Chatrchyan *et al.* (CMS Collaboration), J. High Energy Phys. 11 (2012) 080.
[25] S. Chatrchyan *et al.* (CMS Collaboration), J. High Energy Phys. 07 (2013) 116.
[26] G. Aad *et al.* (ATLAS Collaboration), Phys. Lett. B **749**, 242 (2015).
[27] V. P. Goncalves and C. A. Bertulani, Phys. Rev. C **65**, 054905 (2002).
[28] V. P. Goncalves, B. D. Moreira, and F. S. Navarra, Phys. Rev. C **90**, 015203 (2014); V. P. Goncalves, B. D. Moreira, and F. S. Navarra, Phys. Lett. B **742**, 172 (2015).
[29] V. P. Goncalves and W. K. Sauter, Phys. Rev. D **91**, 035004 (2015).
[30] N. Arkani-Hamed, T. Han, M. Mangano, and L. T. Wang, Phys. Rep. **652**, 1 (2016).
[31] C. A. Bertulani, Phys. Rev. C **79**, 047901 (2009).
[32] V. P. Goncalves, D. T. Da Silva, and W. K. Sauter, Phys. Rev. C **87**, 028201 (2013).
[33] V. P. Goncalves and M. L. L. da Silva, Phys. Rev. D **89**, 114005 (2014).
[34] T. Branz, T. Gutsche, and V. E. Lyubovitskij, Phys. Rev. D **80**, 054019 (2009).
[35] T. Branz, T. Gutsche, and V. E. Lyubovitskij, Phys. Rev. D **82**, 054010 (2010).
[36] T. Branz, R. Molina, and E. Oset, Phys. Rev. D **83**, 114015 (2011).
[37] X. Li and M. B. Voloshin, Phys. Rev. D **91**, 114014 (2015).
[38] G. Baur and L. G. Ferreira Filho, Nucl. Phys. **A518**, 786 (1990).
[39] M. Klusek-Gawenda and A. Szczurek, Phys. Rev. C **82**, 014904 (2010).
[40] V. P. Goncalves, B. D. Moreira, and F. S. Navarra, Eur. Phys. J. C **76**, 103 (2016).
[41] V. P. Goncalves, B. D. Moreira, and F. S. Navarra, Eur. Phys. J. C **76**, 388 (2016).
[42] J. D. Jackson, *Classical Electrodynamics* (John Wiley, New York, 1991).
[43] F. E. Low, Phys. Rev. **120**, 582 (1960).
[44] K. A. Olive *et al.* (Particle Data Group), Chin. Phys. C **38**, 090001 (2014) and 2015 update.